

Entropy-Triggered Retraining as Nonequilibrium Entropy Production in Deployed Machine Learning Systems

Lennon J. Shikhman*

Abstract. Machine learning models deployed in nonstationary environments inevitably experience performance degradation due to data drift. While numerous drift detection heuristics exist, most lack a dynamical interpretation and offer limited guidance on how retraining should be balanced against operational cost. In this work, we propose an entropy-based retraining framework grounded in nonequilibrium statistical physics. Modeling drift as probability flow governed by a Fokker–Planck equation, we quantify model–data mismatch using a time-evolving Kullback–Leibler divergence. We show that its rate of change admits an entropy-balance decomposition featuring a nonnegative entropy production term driven by probability currents. Guided by this theory, we evaluate entropy-triggered retraining in a controlled nonstationary classification setting and demonstrate near-maximum-frequency baseline predictive performance while reducing retraining frequency by an order of magnitude relative to daily and label-based strategies.

Key words. Mathematical machine learning, Fokker–Planck equations, relative entropy, Lyapunov functionals, data drift, stochastic processes, nonequilibrium dynamics

1. Introduction. Machine learning models deployed in real-world environments operate under the implicit assumption that training and deployment data are drawn from the same distribution. In practice, this assumption is routinely violated. Changes in population behavior, sensing mechanisms, feedback effects, or external conditions induce data drift, leading to gradual or abrupt degradation in predictive performance across applications ranging from finance and healthcare to recommender systems and autonomous decision-making.

Despite its prevalence, data drift is often treated primarily as a detection problem rather than a decision problem. Common monitoring strategies, such as heuristic distributional tests, confidence-based alarms, or delayed accuracy feedback, typically answer the question of whether a change has occurred, but provide limited guidance on when retraining is warranted and how retraining frequency should be balanced against operational cost. In deployed systems, retraining incurs nontrivial expense in computation, data labeling, validation, and organizational overhead. As a result, overly sensitive triggers lead to excessive retraining, while conservative policies permit degradation to accumulate.

This paper takes a different point of view. We treat deployment as an evolving stochastic system whose feature distribution changes in time. From this perspective, the central object is not a particular alarm statistic, but the dynamics by which the deployment-time data distribution drifts away from the distribution implicitly encoded by a fixed deployed model. Nonequilibrium statistical physics provides a principled framework for describing irreversible processes through entropy production and probability flow: stochastic dynamics generate probability currents that drive systems away from reference states, producing entropy in the process. Central to this theory is the Fokker–Planck equation, which governs the evolution of probability densities and admits entropy-based functionals that quantify irreversibility.

* Department of Mathematics and Systems Engineering, Florida Institute of Technology (lshikhman2022@fit.edu).

The modern theory of irreversible processes and entropy production originates in the foundational work of Onsager, which established reciprocity relations and identified entropy production as a structural feature of nonequilibrium systems [4]. Subsequent developments formalized the role of probability currents in driving irreversibility and entropy generation in stochastic systems [6]. Within this framework, entropy production is not an incidental artifact of noise, but a consequence of persistent probability flow away from equilibrium.

We leverage this framework to reinterpret model degradation under drift as an entropy-producing dynamical process. Specifically, we model the deployment-time data distribution as a probability flow and quantify model–data mismatch using relative entropy. This yields a label-free signal that is tied directly to the dynamics of drift. Retraining then becomes an intervention that resets the reference distribution associated with the deployed model, reducing accumulated mismatch at an operational cost. This viewpoint motivates entropy-triggered retraining policies that balance predictive performance against retraining frequency by responding to the underlying probability flow rather than to delayed label-dependent performance collapse.

Contributions. The contributions of this work are threefold:

- We provide a dynamical interpretation of model degradation under data drift as nonequilibrium entropy production governed by Fokker–Planck probability flow.
- We establish a relative-entropy mismatch functional whose evolution is driven by probability currents, motivating entropy-triggered retraining as a principled, label-free intervention strategy.
- We empirically demonstrate that entropy-triggered retraining achieves near-maximum-frequency baseline predictive performance while reducing retraining frequency by an order of magnitude relative to daily and label-based retraining strategies.

Organization. Section 2 introduces a probability-flow model of drift. Section 3 defines mismatch entropy and derives its evolution along the flow. Section 4 interprets retraining as an external control that resets mismatch. Section 5 evaluates entropy-triggered retraining experimentally. Appendix A provides the entropy-balance derivation.

2. Drift as Probability Flow. Let $X_t \in \mathbb{R}^d$ denote the feature vector observed at deployment time t . We model its evolution by the stochastic differential equation

$$(2.1) \quad dX_t = a(X_t, t) dt + B(X_t, t) dW_t,$$

where a is a drift field, B a diffusion matrix, and W_t standard Brownian motion.

Under standard regularity assumptions, the probability density $p(x, t)$ of X_t satisfies the Fokker–Planck equation

$$(2.2) \quad \partial_t p(x, t) = -\nabla \cdot J(x, t),$$

where the probability current is given by

$$(2.3) \quad J(x, t) = a(x, t)p(x, t) - \nabla \cdot (D(x, t)p(x, t)), \quad D = \frac{1}{2}BB^\top.$$

The Fokker–Planck equation provides a canonical description of the evolution of probability densities under stochastic dynamics and admits a rich analytical structure; see [5] for a comprehensive treatment.

Nonzero probability currents correspond to nonequilibrium dynamics and provide a mechanism by which a fixed deployed model becomes misaligned with its environment. From the perspective of nonequilibrium statistical physics, such currents are fundamental drivers of irreversibility and entropy production, encoding sustained deviations from equilibrium through persistent probability flow [6].

3. Mismatch Entropy as a Lyapunov Functional. We quantify model–data mismatch using the relative entropy

$$(3.1) \quad D(t) = D_{\text{KL}}(p(\cdot, t) \parallel q_{\text{ref}}),$$

which measures the statistical divergence between the evolving deployment-time data distribution $p(x, t)$ and the fixed reference distribution associated with the deployment environment. From an information-theoretic perspective, relative entropy provides a natural and asymmetric measure of distributional mismatch that is independent of labels or model outputs [1].

Differentiating $D(t)$ along the Fokker–Planck flow yields

$$(3.2) \quad \frac{d}{dt} D(t) = \int_{\mathbb{R}^d} J(x, t) \cdot \nabla \log \frac{p(x, t)}{q_{\text{ref}}(x)} dx,$$

where boundary terms are assumed to vanish. This identity makes explicit that the temporal evolution of mismatch is driven by probability currents in feature space induced by drift.

In reversible settings where the reference density aligns with a stationary distribution of the flow, relative entropy acts as a Lyapunov functional and dissipates along the dynamics. More generally, along nonequilibrium probability flows the entropy rate admits a decomposition analogous to the entropy balance relation of stochastic thermodynamics, featuring a nonnegative entropy production term driven by probability currents and a residual “housekeeping” term that captures sustained driving. Such entropy balance relations play a central role in stochastic thermodynamics for diffusion processes [7], and closely related variational structures for Fokker–Planck dynamics are developed in [3]. The full derivation of the decomposition used here is provided in Appendix A.

Remark 1 (Lyapunov and nonequilibrium interpretation). *When q_{ref} coincides with an appropriate stationary reference for the flow, the mismatch entropy $D(t)$ behaves as a Lyapunov functional and decays monotonically. Under driven nonequilibrium drift, $D(t)$ need not be monotone; nevertheless, its evolution is constrained by an entropy-balance relation with a nonnegative entropy production term, and increases in mismatch reflect the effect of sustained probability currents relative to the fixed deployed reference distribution.*

This distinction matters operationally. Loss-based retraining triggers are necessarily reactive because they depend on labels and respond only after predictive performance has already degraded. In contrast, mismatch entropy is a property of the deployment-time feature distribution and can provide an early warning signal in settings where feature-space drift correlates with predictive risk (e.g., under covariate shift), indicating when retraining may become necessary before substantial performance degradation is observed.

From mismatch to intervention. Sections 2–3 provide a simple implication: if the deployment-time distribution evolves under probability currents, then mismatch relative to a fixed deployed

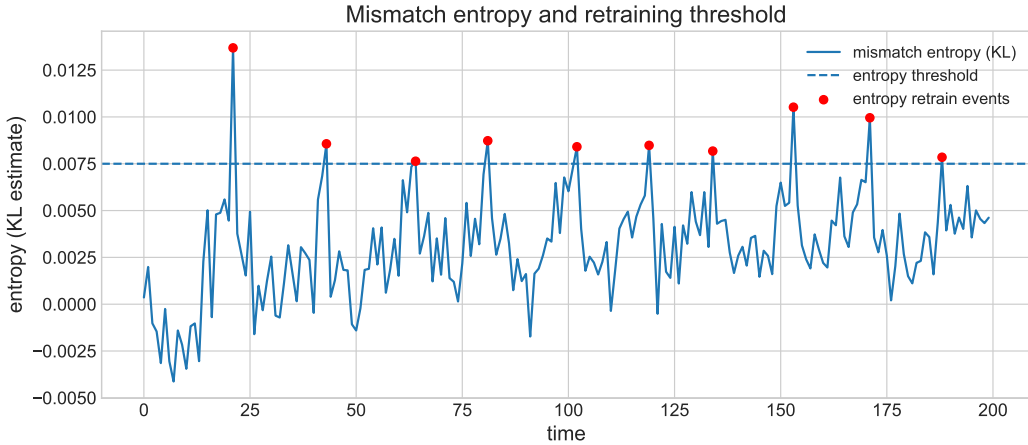


Figure 3.1. Evolution of mismatch entropy under nonstationary drift. The threshold defines entropy-triggered retraining events. Small negative empirical values arise from finite-sample estimation noise; the population Kullback–Leibler divergence is nonnegative.

reference will generally change over time, and sustained drift produces nonequilibrium entropy production. Maintaining predictive performance therefore requires an intervention that updates the deployed reference. In deployed learning systems, this intervention is retraining.

4. Retraining as External Work. Retraining corresponds to resetting the reference distribution q_{ref} by incorporating newly observed data, thereby reducing accumulated mismatch entropy at the cost of computation, data acquisition or labeling, validation, and operational disruption. This mirrors the role of external work in nonequilibrium statistical physics, where entropy reduction requires resources supplied by an external agent.

From this perspective, retraining policies act as control strategies. Frequent retraining applies external work continuously, maintaining low mismatch at maximal operational cost, while infrequent retraining allows mismatch to accumulate and may permit performance to degrade beyond acceptable levels. Fixed schedules apply intervention independently of the underlying drift dynamics, whereas loss-triggered policies react only after degradation has already occurred.

Entropy-triggered retraining occupies an intermediate regime. By monitoring $D(t)$ (or a consistent estimator of it), retraining is initiated only when accumulated mismatch exceeds a tolerable threshold. This yields a principled tradeoff between predictive performance and retraining cost, applying external work selectively in response to the probability flow rather than to delayed performance signals.

5. Experimental Evaluation.

5.1. Setup. We evaluate retraining strategies in a controlled binary classification task under synthetic nonstationarity. A logistic regression model is trained on an initial Gaussian feature distribution and deployed on a data stream with gradually shifting mean, increasing variance, and a rotating decision boundary.

We compare the following retraining strategies:

- No retraining,
- Daily retraining (maximum-frequency baseline),
- Weekly retraining,
- Performance-triggered retraining (label-based),
- Entropy-triggered retraining (KL-based, label-free).

Retraining cost is measured by the number of retraining events, and predictive performance is measured by log loss.

5.2. Results. Figure 5.1 shows predictive log loss over time under drift. As expected, the model without retraining steadily degrades. Daily retraining provides a maximum-frequency baseline, keeping loss low at the cost of frequent retraining. Entropy-triggered retraining closely tracks the daily maximum-frequency baseline with far fewer retraining events, indicating that the mismatch signal provides actionable advance warning.

Table 5.1 summarizes the performance–cost tradeoff. In this experiment, entropy-triggered retraining achieves average log loss within about one percent of daily retraining while reducing retraining count from 199 to 10 (roughly a 95% reduction). Performance-triggered retraining achieves near-maximum-frequency baseline loss but retrains far more frequently, illustrating the operational burden of label-dependent reactive policies.

Figure 5.2 visualizes cumulative retraining counts over time. Daily and performance-triggered approaches incur near-continuous retraining, whereas entropy-triggered retraining concentrates interventions at a small number of drift-driven times. Finally, Figure 5.3 provides a Pareto view: entropy-triggered retraining lies close to the efficient frontier, offering near-maximum-frequency baseline performance at substantially reduced cost.

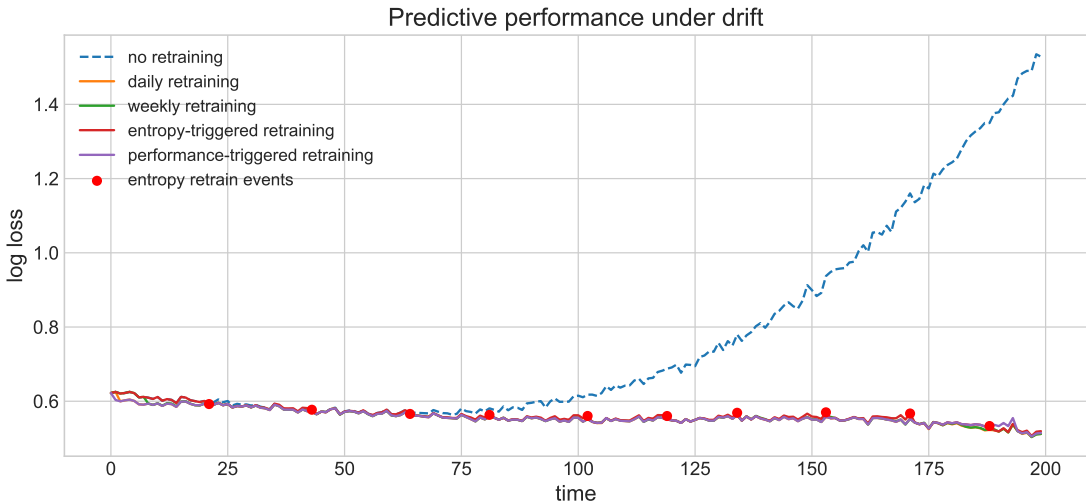


Figure 5.1. Predictive log loss over time under nonstationary drift for different retraining strategies. Entropy-triggered retraining tracks daily retraining while requiring far fewer interventions.

Method	Avg Log Loss	Worst Log Loss	Final Log Loss	# Retrains
No retraining	0.7716	1.5351	1.5286	0
Daily retraining	0.5586	0.6251	0.5118	199
Weekly retraining	0.5595	0.6252	0.5119	28
Entropy-triggered	0.5626	0.6252	0.5193	10
Performance-triggered	0.5592	0.6221	0.5144	138

Table 5.1
Predictive performance and retraining cost under nonstationary drift.

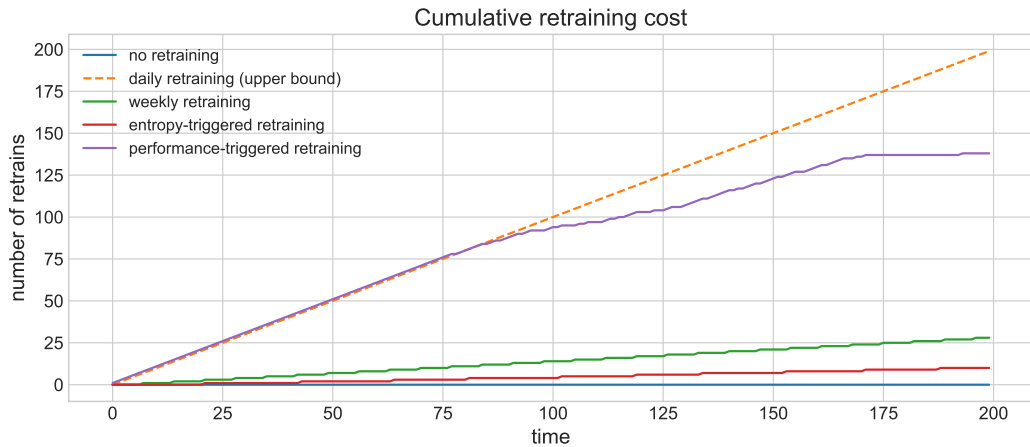


Figure 5.2. Cumulative number of retraining events over time. Entropy-triggered retraining reduces retraining frequency by an order of magnitude relative to daily and performance-triggered baselines.

6. Discussion. These results support the theoretical interpretation of model degradation as a nonequilibrium process driven by probability currents. Unlike heuristic drift metrics, mismatch entropy is tied directly to the dynamics of the deployment-time distribution and provides a principled handle for balancing predictive performance against retraining cost.

From a geometric viewpoint, relative entropy also admits an interpretation as a divergence on statistical manifolds, further supporting its role as a structural measure of model–data mismatch [2]. Practically, the main limitations concern estimation of mismatch entropy in high-dimensional settings and the choice of threshold. These are not unique to the proposed approach: any operational retraining policy requires selecting a tolerable performance–cost operating point. The advantage of entropy-triggered monitoring is that it connects this choice to an interpretable dynamical quantity driven by probability flow.

7. Conclusion. We presented a theory-driven retraining framework that interprets model degradation under data drift as nonequilibrium entropy production. Modeling drift as Fokker–Planck probability flow yields a mismatch-entropy functional whose evolution is driven by probability currents and admits an entropy-balance decomposition with a nonnegative entropy production term. This provides a principled, label-free monitoring signal for deciding when

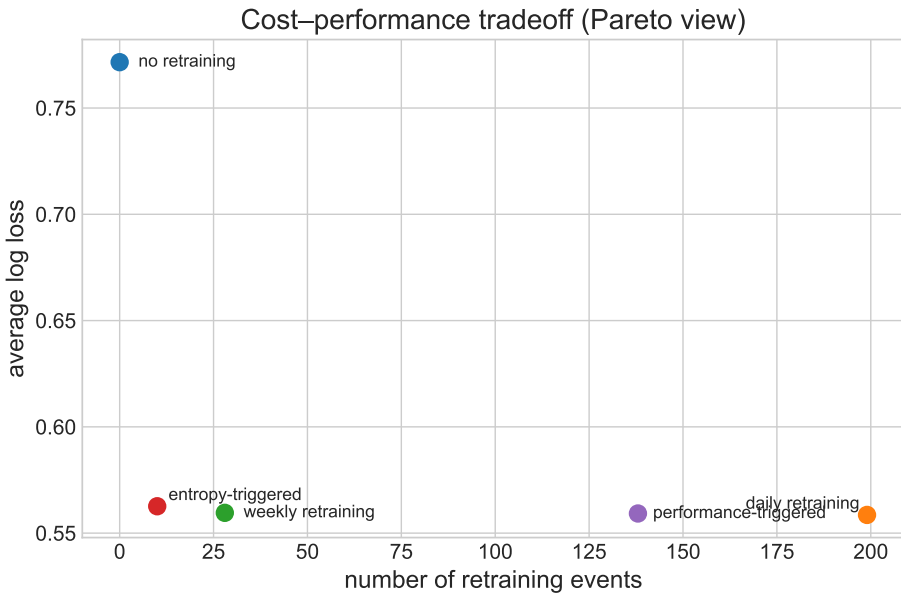


Figure 5.3. Cost–performance tradeoff (Pareto view). Each point corresponds to a policy, with cost measured by the number of retraining events and performance measured by average log loss.

retraining becomes necessary. Experiments demonstrate that entropy-triggered retraining achieves near-maximum-frequency baseline performance at a fraction of the retraining cost.

Appendix A. Proof of the Entropy Production Decomposition. In this appendix we derive the decomposition of the time derivative of the model mismatch entropy that underlies the entropy-triggered retraining framework. The structure of the result parallels entropy-balance relations in stochastic thermodynamics for diffusion processes. Related connections between entropy dissipation, diffusion, and variational structure are developed extensively in the optimal transport literature [8].

Let $p(x, t)$ be a probability density on \mathbb{R}^d evolving according to the Fokker–Planck equation

$$(A.1) \quad \partial_t p(x, t) = -\nabla \cdot J(x, t),$$

with probability current

$$(A.2) \quad J(x, t) = a(x, t)p(x, t) - \nabla \cdot (D(x, t)p(x, t)),$$

where $a(x, t)$ is a drift field and $D(x, t)$ is a symmetric positive definite diffusion tensor almost everywhere.

Let $q_{\text{ref}}(x)$ be a fixed reference density satisfying $q_{\text{ref}}(x) > 0$ wherever $p(x, t) > 0$, and define the associated potential

$$(A.3) \quad U_\theta(x) = -\log q_{\text{ref}}(x).$$

We assume that:

- $p(\cdot, t)$ is smooth and integrable for each t ,
- either $p(x, t) > 0$ almost everywhere or $J = 0$ on the set $\{p = 0\}$,
- boundary terms vanish so that integration by parts is valid.

The model mismatch entropy is defined as

$$(A.4) \quad D(t) = D_{\text{KL}}(p(\cdot, t) \| q_{\text{ref}}) = \int_{\mathbb{R}^d} p(x, t) \log \frac{p(x, t)}{q_{\text{ref}}(x)} dx.$$

Differentiating with respect to time and using the continuity equation $\partial_t p = -\nabla \cdot J$, we obtain

$$(A.5) \quad \frac{d}{dt} D(t) = \int_{\mathbb{R}^d} \partial_t p(x, t) \log \frac{p(x, t)}{q_{\text{ref}}(x)} dx$$

$$(A.6) \quad = - \int_{\mathbb{R}^d} \nabla \cdot J(x, t) \log \frac{p(x, t)}{q_{\text{ref}}(x)} dx.$$

Integrating by parts and discarding boundary terms yields

$$(A.7) \quad \frac{d}{dt} D(t) = \int_{\mathbb{R}^d} J(x, t) \cdot \nabla \log \frac{p(x, t)}{q_{\text{ref}}(x)} dx.$$

Using the definition of U_θ , we write

$$(A.8) \quad \nabla \log \frac{p}{q_{\text{ref}}} = \frac{\nabla p}{p} + \nabla U_\theta.$$

In the Itô formulation, the probability current satisfies

$$(A.9) \quad J = ap - \nabla \cdot (Dp) = [a - (\nabla \cdot D)]p - D\nabla p.$$

Solving for $\nabla p/p$, we obtain

$$(A.10) \quad \frac{\nabla p}{p} = D^{-1} [a - (\nabla \cdot D)] - \frac{D^{-1} J}{p}.$$

Substituting this expression into the entropy rate identity yields

$$(A.11) \quad \frac{d}{dt} D(t) = \int_{\mathbb{R}^d} J(x, t) \cdot \left(D^{-1} [a - (\nabla \cdot D)] + \nabla U_\theta \right) dx - \int_{\mathbb{R}^d} \frac{J(x, t)^\top D^{-1} J(x, t)}{p(x, t)} dx.$$

We define the total entropy production rate as

$$(A.12) \quad \dot{\Sigma}_{\text{tot}}(t) := \int_{\mathbb{R}^d} \frac{J(x, t)^\top D(x, t)^{-1} J(x, t)}{p(x, t)} dx,$$

and group the remaining contribution into a housekeeping term $\dot{Q}_{\text{hk}}(t)$.

Thus, the mismatch entropy satisfies the decomposition

$$(A.13) \quad \frac{d}{dt} D(t) = -\dot{\Sigma}_{\text{tot}}(t) + \dot{Q}_{\text{hk}}(t).$$

Since $D(x, t)$ is symmetric positive definite, its inverse $D^{-1}(x, t)$ is also positive definite. Consequently,

$$(A.14) \quad J(x, t)^\top D(x, t)^{-1} J(x, t) \geq 0$$

pointwise, and division by $p(x, t) > 0$ preserves this inequality. Hence,

$$(A.15) \quad \dot{\Sigma}_{\text{tot}}(t) \geq 0,$$

with equality if and only if $J(x, t) \equiv 0$, corresponding to equilibrium dynamics.

This establishes nonnegativity of the entropy production term in the mismatch-entropy balance relation used in the main text.

Acknowledgements.

AI Use Disclosure. The author used an artificial intelligence language model (ChatGPT, OpenAI; accessed December 29–31, 2025) as an assistive tool during manuscript preparation. The tool was used for expository editing and LaTeX formatting, limited symbolic checks of intermediate algebraic steps, and code drafting for experimental pipelines and figures. All mathematical derivations, modeling choices, experiments, and interpretations were independently derived, executed, and verified by the author.

Reproducibility. Computational experiments were conducted using a Jupyter notebook and a conda-managed Python environment. The notebook and environment specification can be shared upon request.

Acknowledgement of Computational Resources. The author gratefully acknowledges the use of a Dell Pro Max workstation for conducting the computational experiments reported in this work.

REFERENCES

- [1] T. M. COVER AND J. A. THOMAS, *Elements of Information Theory*, Wiley, 2nd ed., 2006.
- [2] S. ICHI AMARI, *Information Geometry and Its Applications*, Springer, 2016.
- [3] R. JORDAN, D. KINDERLEHRER, AND F. OTTO, *The variational formulation of the fokker–planck equation*, SIAM Journal on Mathematical Analysis, 29 (1998), pp. 1–17, <https://doi.org/10.1137/S00361414096303359>.
- [4] L. ONSAGER, *Reciprocal relations in irreversible processes*, Physical Review, 37 (1931), pp. 405–426, <https://doi.org/10.1103/PhysRev.37.405>.
- [5] H. RISKEN, *The Fokker–Planck Equation: Methods of Solution and Applications*, Springer, 2nd ed., 1989.
- [6] J. SCHNAKENBERG, *Network theory of microscopic and macroscopic behavior of master equation systems*, Reviews of Modern Physics, 48 (1976), pp. 571–585, <https://doi.org/10.1103/RevModPhys.48.571>.
- [7] U. SEIFERT, *Entropy production along a stochastic trajectory and an integral fluctuation theorem*, Physical Review Letters, 95 (2005), p. 040602, <https://doi.org/10.1103/PhysRevLett.95.040602>.
- [8] C. VILLANI, *Topics in Optimal Transportation*, American Mathematical Society, 2003.